AIAA JOURNAL
Vol. 43, No. 4, April 2005

Experimental Study of Incompressible Jets with Different Initial Swirl Distributions: Mean Results

R. T. Gilchrist* and J. W. Naughton†
University of Wyoming, Laramie, Wyoming 82071

Incompressible swirling jets with Reynolds numbers of 1.0×10^5 have been studied using a miniature five-hole probe. The jet facility in which these measurements have been made has been specifically designed to produce a highly conditioned, swirling jet flow. To provide a comprehensive investigation of the effect of low-to-moderate swirl (well below vortex breakdown) on jet growth rate, two tangential velocity profiles, a solid-body type and a q-vortex type with swirl numbers of both 0.10 and 0.23, have been investigated and compared with a nonswirling jet. The different tangential velocity distributions appear to have a minimal effect on the growth-rate enhancement observed. In contrast, the swirl number does affect growth rate enhancement (up to ∼40% for the cases studied), but only when it exceeds a certain level. This result contradicts some earlier studies that assumed a linear increase in growth rate with swirl, but supports the results from newer studies. These newer results suggest three regimes for swirl-enhanced growth rates: 1) low swirl levels where no enhancement occurs, 2) moderate swirl levels where the enhancement scales with the swirl number, and 3) high swirl levels where vortex breakdown dominates the process.

Nomenclature

a	=	constant in sech^2 distribution; constant in the centerline velocity decay relationship
b	=	jet half-width
$b' = \mathrm{d}b/\mathrm{d}x$	=	jet growth rate
C_p	=	pressure coefficient
C_{pitch}, C_{yaw}	=	five-hole calibration constants
D	=	nozzle-exit diameter
G_z	=	axial momentum
G_θ	=	axial component of angular momentum
k	=	circulation
k_t	=	characteristic circulation
P	=	mean static pressure
P_a	=	ambient pressure
R	=	nozzle exit radius
r_t	=	characteristic radius
S	=	swirl number
s	=	constant in the centerline velocity decay relationship
U_p	=	uncertainty in probe pressure
$U_o = 50$ m/s	=	average exit axial velocity
u, v, w	=	Cartesian velocity components
$\bar{u}, \bar{v}, \bar{w}$	=	mean Cartesian velocity components
v_x, v_r, v_θ	=	cylindrical velocity components
x, r, θ	=	cylindrical coordinate system
x, y, z	=	Cartesian coordinate system
ρ	=	air density

Subscripts

c	=	centerline
hw	=	based on velocity width
m	=	based on momentum width
max	=	maximum value
o	=	nozzle exit

Presented as Paper 2003-0639 at the AIAA 41st Aerospace Sciences Meeting, Reno, NV, 6–9 January 2003; received 14 August 2003; revision received 18 October 2004; accepted for publication 18 October 2004.

*Graduate Research Assistant, Department of Mechanical Engineering.
†Associate Professor, Department of Mechanical Engineering. Associate Fellow AIAA.

Introduction

SWIRLING jet flows are used in many applications including combustion and separation control as a result of their unique flowfield properties. In addition, swirling jet flows are byproducts of flows through turbomachinery and flows over wings. Despite their prevalence, some aspects of swirling jet flows are not well understood. For example, swirling jet flows exhibit increased growth rates compared to pure axial-flow jets (see, for example, Farokhi et al.[1] and Naughton et al.[2]), but the mechanism behind the increased growth has yet to be conclusively demonstrated.

One of the variables affecting growth rates in swirling flows that is not well understood is the initial swirl profile at the jet exit. Only one previous experimental study has investigated an unconfined jet with multiple swirl profiles,[3] and that has only been done at one swirl strength. Recently, direct numerical simulation[4,5] and linear stability theory[6,7] have been used to compare different tangential velocity profiles. However, the generation of several different swirl profiles in an experimental facility is not easily accomplished. For instance, rotating pipes produce only one type of swirl profile, and vane systems require a change of vane geometry to produce different flows.

The primary goal of this paper is to investigate the combined effect of initial swirl profile and swirl strength on jet growth rates using mean flowfield measurements in the near field and the developing region of a jet flow. The careful design of the experiment carried out here has eliminated potential facility-induced artifacts that might have affected the results from some previous studies. The results reported here are part of a larger study investigating the mechanisms behind the enhanced growth rate observed in swirling jets and their exploitation for actively controlling jet flows. Details of the fluctuating flowfield and turbulent structure of the swirling jets studied here will be the subject of later publications.

To generate the different swirl profiles investigated in this study, a unique facility which allows for fine control of the tangential velocity profile and the creation of a swirling jet that is largely free from artifacts produced by the swirl generation process, has been designed and constructed, Gilchrist and Naughton[8] provide a detailed description of this facility. In the initial stage of this study, several swirl profiles were explored from which the two most distinct profiles were chosen for further study. These two profiles, one resembling an Oseen vortex or a q vortex (solid-body core with a

free vortex outer region) and the other resembling solid-body rotation, have been generated with two different swirl numbers that are well below that necessary for vortex breakdown. Mean velocity measurements of these four swirling flows and the nonswirling jet have been obtained at axial locations from the nozzle exit to almost 20 diameters downstream using a miniature five-hole probe. The primary finding in this study is that the addition of swirl to a jet flow increases the growth rate independent of the initial swirl profile provided the swirl strength is sufficiently large.

Previous Work

The current study builds upon a large number of previous investigations of swirling jet flows. A recent comprehensive review of swirling jet flows is not available and is not attempted here. Rather, only those studies most relevant to the current investigation are discussed. A more general overview of swirling jet flows can be found in several texts (for examples, see Refs. 9 and 10). Although there are many studies of swirling jet flows, there are few studies that have investigated incompressible swirling freejets over the range of conditions and in the detail provided by the present study.

It has been known for a long time that imposing an additional component of strain on a turbulent flow produces larger changes to the flow than would be predicted by the simple increase in total strain.[11] For instance, imposing curvature on a turbulent boundary layer has an order-of-magnitude greater effect on skin friction than does the same curvature acting on a laminar boundary layer. These results are attributed to the additional terms that appear in the equations of motion, particularly the Reynolds-stress equation, and it has been suggested that curvature causes changes in the turbulence structure.[11] These observations suggest that adding a component of strain to a jet that is in a direction perpendicular to the strain produced by the jet's axial velocity should cause a large change in the observed jet growth rate. A convenient means of producing this additional strain in a round jet is the addition of azimuthal momentum thereby producing a swirling jet flow. In addition to producing extra strain, swirling jets impose pressure gradients on the flow that are required to support the flow curvature in the jet.

Based on similar reasoning and experimental evidence suggesting enhanced growth rates in swirling jets, many studies in swirling jet flows have been undertaken. Measurements have been made in jets with solid-body-type swirl distribution[12,13] and a swirl distribution with a solid-body core and an outer region that decays with radius.[2,14–16] Measurements have also been obtained in both the region near the swirling jet exit[2,13,15] and in the region downstream of the initial development.[12,14,17] In addition to these incompressible studies, the effect of swirl on compressible jet growth rates has been studied.[2,16] All of the studies just quoted have been conducted in unconfined swirling jets, but confined swirling jets have also been studied.[18] Swirling flows have also been widely studied for their use in combustion applications.[19] In an experiment similar to that performed here, Farokhi et al.[3] studied swirling jet flows with different initial swirl profiles but with a constant swirl number. The two swirl distributions on which they focused were a solid-body distribution (tangential velocity proportional to radius) and a distribution with a solid-body type core and a free vortex (tangential velocity proportional to the inverse of the radius) outer region, henceforth referred to as a q vortex. Both of these jets exhibited an axial velocity profile with the peak velocity on the centerline. From these many studies, several consistent observations have been made, and some understanding of swirling jet flows has been gained. In most cases, the experimental results have shown that swirling jets exhibit more rapid growth than their nonswirling counterparts. This enhanced growth has been attributed to the centrifugal instability present in these swirling jets that enhances the streamwise vorticity present in the mixing layer.[13] The enhanced growth has also been shown to be well correlated with the Richardson number[16] and to scale with increasing tangential velocity at the mixing layer boundary.[2] The effect of swirl also increases with compressibility, which has been attributed to the increased importance of the streamwise vortices as the effect of azimuthal vorticity (i.e., the Kelvin–Helmholtz vortices) diminishes.[2] Another result is that, unlike other enhancement methods that can cause local increases in growth rate, swirl produces enhancement over a large axial extent.

Swirling jet flows have also been studied using linear stability analysis and computational simulations, including both Reynolds-averaged Navier–Stokes and direct-numerical-simulation (DNS) approaches. Linear stability studies include inviscid temporal,[20] viscous temporal,[21,22] viscous compressible temporal,[23] inviscid spatial,[1,6,7] viscous spatial,[24] and inviscid compressible spatial[25] stability. Tangential velocity profiles that have been studied include solid-body rotation (Rankine type),[6] q vortex (Batchelor or Oseen type),[7,20,26] Görtler vortex,[23] and profiles with tangential velocity concentrated in the shear layer.[24,25] The results of these studies indicate that swirl destabilizes jet flows. Such flows exhibit amplified negative helical modes (modes travelling in a direction opposite to the mean swirl) and are unstable to a wider range of disturbances than their nonswirling counterparts. The inviscid analyses indicate that all negative helical modes are unstable, whereas viscous results show that the higher modes are stabilized by viscosity.[21] Unique viscous modes are also present, showing the viscosity can have a destabilizing influence, but the growth rates of these modes are orders of magnitude smaller than the inviscid modes.[22] The results are also consistent in showing that there is a swirl number above which all modes are stabilized. This implies that there is an optimum swirl where one mode exhibits the maximum growth rate, but the optimum swirl varies among the studies. The spatial studies also indicate that the negative helical modes are unstable over a range of swirl and that there is an optimum swirl at which growth rate is a maximum. In addition, the spatial studies reveal that there is a range of swirl over which the instability transitions from convective instability to absolute instability regardless of swirl profile.[7,26] For a nonswirling jet, this transition requires counterflow, whereas, for swirling jets, the flow can be absolutely unstable even in the presence of a small coflow. The studies that considered isolated swirl in the mixing layer have indicated that the additional component of shear is the important contribution to the enhanced growth rates observed. The growth rates of the centrifugal instabilities are significantly dampened as the swirl decays,[24] and swirl shear provides the source for the disturbance energy.[25] Finally, the compressible studies indicate that the growth rate enhancement caused by swirl continues in the compressible regime,[25] and the damping effect of compressibility observed in nonswirling jets is either reduced or nonexistent for some negative helical modes.[23] Although the results of these studies provide insight into possible mechanisms for enhancement, they are only valid in the linear regime, which limits their applicability.

Computational simulations have been performed for swirling jet flows to assess turbulence models[27] as well as to investigate possible mechanisms behind the increased growth rates observed.[4,5] Temporal simulations have been performed for axial profiles with both an Oseen vortex (q-vortex) tangential velocity profile and a Taylor vortex tangential profile. This latter vortex has a solid-body core that transitions to a tangential velocity profile that decays faster with radius than either the q vortex or the Görtler vortex and is chosen because it is centrifugally unstable. For the Oseen vortex tangential profile, the results show that, for small time, the simulations agree well with predictions from linear stability theory. At a later time, interaction between the axisymmetric mode and jet swirl causes outward movement of vortex pairs that significantly enhance the simulated jet's growth rate. This nonlinear interaction between the jet swirl and the azimuthal vortices produced by instability cannot be predicted by linear stability theory. One helical mode has also been investigated for this vortex and is found to produce three-dimensional vortical structures that break down for later times as a result of combined axial and azimuthal stretching. The outward movement of vortical structures is present for the helical mode, but it is somewhat decreased from that observed for the axisymmetric mode. The authors state that these results indicate that an unstable swirl profile is not a necessary condition for jet growth enhancement. This is supported by their later investigation of an unstable profile.[5] Those results show some difference in the interaction of the axisymmetric mode with the swirl, but show no difference when helical disturbances are added.

Table 1 Test cases for the present study

Case number	Swirl type	S	$u_{c,0}$, m/s	$w_{\max,0}$, m/s
1	Nonswirling	0.00	50.4	——
2	q Vortex	0.10	54.2	12.2
3	q Vortex	0.23	61.7	24.5
4	Solid body	0.10	51.2	10.5
5	Solid body	0.23	56.3	21.7

A number of interesting questions that this study intends to address remain unanswered. Although the effect of initial swirl distribution has been experimentally studied by the group from the University of Kansas and NASA Lewis Research Center (see Farokhi et al.[3]), their means of generating the swirl close to the nozzle exit is likely to have produced disturbances in their flow that might have affected the results. Also, conclusive experimental evidence of the modification of the turbulence structure (such as the results from the DNS studies) and the mechanisms causing the turbulence modification are lacking. With a clear knowledge of how swirl enhances growth rate, the enhancement mechanism can be increased or optimized.

Test Cases

The effect of the initial swirl profile and swirl strength on jet growth rates is documented through mean velocity measurements. A list of the test cases is provided in Table 1, where the individual cases have been listed by the type of swirl profile and the swirl number S given by[9,28]

$$S = \frac{G_\theta}{RG_x} = \frac{\int_0^R 2\pi r^2 \rho \bar{u}\bar{w}\,\mathrm{d}r}{R\int_0^R 2\pi r[\rho\bar{u}^2 + (\bar{P} - P_a)]\,\mathrm{d}r} \tag{1}$$

In addition to the swirl number, the centerline axial velocity at the jet exit $u_{c,0}$ and the maximum tangential velocity at the exit $w_{\max,0}$ are given in Table 1. During testing, the flow is adjusted such that the mean axial velocities are the same for all five cases. The Reynolds number based on average nozzle-exit axial velocity and nozzle diameter is 1.0×10^5 for all cases.

The remainder of the paper is organized as follows. First, the facility and instrumentation used to obtain the measurements are discussed. Next, the results of mean flowfield surveys and results determined from them are presented. Finally, the results are discussed, and some conclusions are drawn.

Experimental Setup

Swirling Jet Facility

A specialized flow facility has been used in this study to produce both nonswirling and swirling jets. This facility, shown in Fig. 1, is discussed in detail by Gilchrist and Naughton.[8] The axial and tangential components of the flow are independently controlled by injecting them separately into a stilling chamber. The axial flow is introduced into the end of the stilling chamber using air provided by a regenerative blower and passes through baffle plates to ensure that it is evenly distributed across the chamber. To produce the swirling flow, high-pressure air from a compressor is tangentially injected into the stilling chamber through 32 separate injection points that allow for fine control of the tangential profile. The combined flow then passes through four screens to remove any artifacts and is accelerated through a converging section and a nozzle that provide a 44:1 contraction ratio. The flow conditioning provided by the screens and large contraction have been specifically designed to produce a highly conditioned exit flow. A facility where swirling flow was conditioned by screens and a contraction was used by Wu and Farokhi,[29] but the distance between the screens and the nozzle exit was short.

To calibrate the five-hole probe and to perform automated flowfield surveys, a traverse system that has movement in three Cartesian axes (one of which is computer controlled) and pitch and yaw movement (both of which are computer controlled is used).

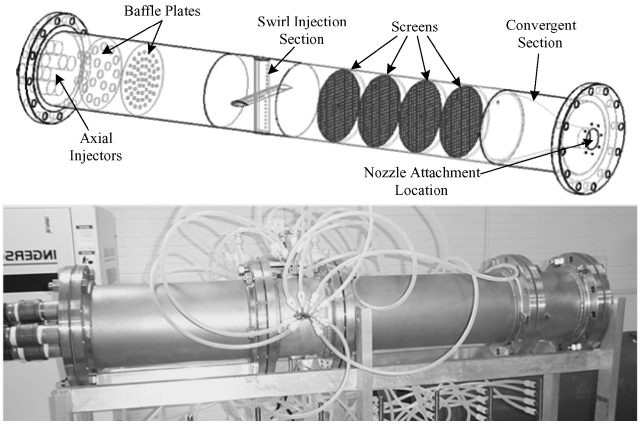

Fig. 1 Swirling jet facility.

The traverse system is discussed in detail in Ref. 8. Probes can be automatically calibrated by centering the probe in a nonswirling jet and using the pitch and yaw controls to systematically change the probe's attitude in the flow. After calibration, the traverse system is used to acquire a flowfield survey across the entire jet once it has been manually centered in the jet at a certain distance away from the jet exit.

Five-Hole Probe

For the mean flow measurements presented here, a miniature five-hole probe is used. A five-hole probe has been chosen for its robust nature, reliable calibration, and for the pressure measurements that it provides in addition to velocity measurements. Five-hole probes have been extensively used in incompressible swirling flows including wing-tip vortices,[30] coflowing jets,[31] and swirling freejets.[3,17] Caution must be exercised when utilizing a probe in a swirling flow because its introduction into the flow can create a local region of vortex breakdown if enough swirl is present. However, the flows investigated in this study do not exhibit reverse flow and have swirl numbers well below those that are generally observed in vortex breakdown, and so probe interference resulting from vortex breakdown is not expected here. As shown in Fig. 2a, a 1.59-mm (1/16-in.)-diam five-hole probe with a hemispherical head is used to provide flowfield measurements with a resolution of 1/24 of the nozzle-exit diameter. The errors resulting from the finite width of the probe are addressed in the Uncertainty section. The pressures from the five-hole probe are measured by a Validyne DP15 differential pressure transducer connected to the probe's multiple pressure ports through a Scanivalve multiplexor. Voltages from the pressure transducer are digitized using a computer controlled A/D board, and the values are stored on a computer for later processing. The relatively long tubing that connects the probe to the pressure transducer creates a large capacitance in the pressure system. Therefore, each time the Scanivalve is switched to a different probe hole, the system is allowed to equalize over 20 s before a pressure reading is taken. The large capacitance in the system also ensures that any short timescales associated with turbulence are averaged out; only mean flowfield measurements are recorded. Motion of the traverse system, monitoring of the conditions in the stilling chamber, and measurement of the five-hole probe pressures for both calibration and flow-field surveys are controlled using a Labview program.

The probe was fully calibrated in the swirling jet facility (in the absence of swirl) over a range of ± 35 deg in pitch and yaw in 5-deg increments. Zilliac's calibration method[32] is used to determine flowfield quantities from the measured pressures. In this approach, five pressures at the probe's tip are recorded at each calibration point. Differences between these five pressures are nondimensionalized by the pressure difference between the central hole and the average of the four surrounding holes. These pressure differences yield local total pressure, static pressure, pitch, and yaw coefficients, two of which are shown in Fig. 2b, that exhibit smooth behavior over the region calibrated. During a survey, the five probe pressures are measured and are used to calculate the nondimensionalized coefficients.

These coefficients are entered into a two-dimensional interpolation program that determines the flowfield quantities. Confidence in utilizing a five-hole probe in the present flows is garnered from past studies that have shown negligible differences in mean measurements made with cross wires and five-hole probes in flowfields containing turbulent intensities of up to 25% (Ref. 30). Indeed, measurements of the velocity at the jet exit in the present study have been performed with a crosswire, and mean profiles essentially identical to those measured with the five-hole probe have been obtained.

Although the five-hole probe has many advantages, it also has limitations. The probe is limited to single point measurements, and its size limits the spatial resolution, which can produce poor results where high gradients exist. In the present configuration, the probe is limited to mean measurements only. The probe is also an intrusive device, a factor that must be considered carefully in swirling flows where the presence of a probe can cause vortex breakdown caused by the pressure field it creates. For the present study, none of these limitations prevents the five-hole probe from making high-quality measurements in the swirling jets.

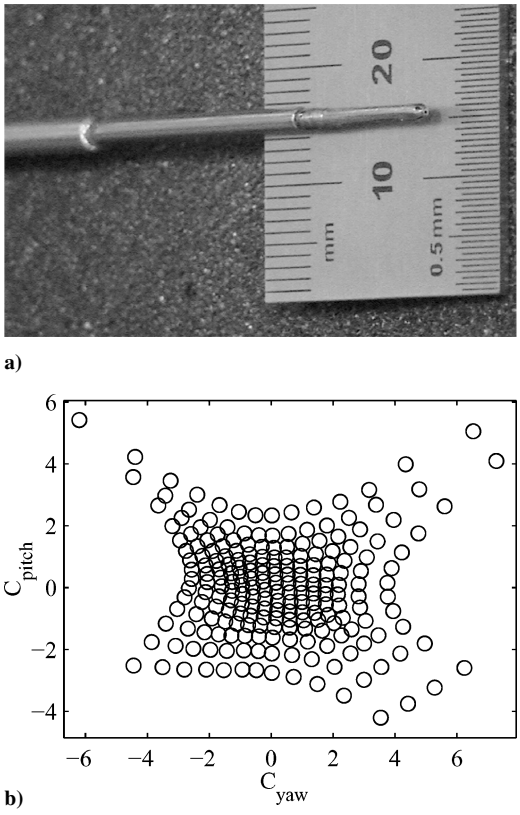

Fig. 2 Five-hole probe: a) image of probe and b) example calibration.

The coordinate systems used in the present study and parameters important to jet flows are given in Fig. 3. At different axial locations x, surveys in y have been performed through the center of the swirling jet flows at $z = 0$. To be consistent with previous measurements in swirling and nonswirling jet flows, the coordinate system used in this study is situated such that, along the traverse direction, the mean axial velocity $\bar{u}$, the mean radial velocity $|\bar{v}|$, and the mean tangential velocity $|\bar{w}|$ are measured as functions of y.

Uncertainty

The uncertainty in the velocities measured by the five-hole probe is primarily driven by the large pressure gradients found in swirling flows and the error in the pressure measurement itself. To determine the magnitude of the uncertainty driven by the pressure gradient, the pressure difference across the radius of the probe (0.8 mm) is calculated using the pressure gradient obtained from the surrounding points. This pressure difference, which is the error caused by the position difference between each tube and the center of the probe, is combined with the uncertainty in the pressure measurement, and the result is assumed to be the maximum pressure uncertainty $U_{p,\max}$ at each tube in the probe. To determine the effect of the pressure uncertainty on the velocity, the following approach is taken. A random pressure uncertainty $0 < U_p < U_{p,\max}$ is applied to each of the five pressures, and a new value for the velocity is calculated. This process is repeated 100 times for each point, and a representative uncertainty in the velocity measurement is determined from the 100 different velocity values. Figure 4 shows the velocity profiles of the five cases at the jet exit and includes error bars to demonstrate the magnitude of pressure error. As expected, the uncertainties are greatest in the regions of high pressure gradient and in locations where the measured pressures are low.

Because the traverse system utilizes stepper motors with high-precision optical encoders and a worm drive with no backlash to drive the y axis, uncertainties in the position are on the order of a 0.05 mm and are therefore not included in Fig. 4.

The swirl number is determined by integrating the velocity and pressure profiles taken close to the jet exit. Uncertainties in the swirl number were estimated by propagating the uncertainty in the velocity at the nozzle exit through the numerical integration. The uncertainties in the swirl numbers are reported in the Results section.

Results

Velocity and Pressure Profiles

Exit Velocity Profiles

The first step in this study was to create the five different swirling flows listed in Table 1 at the nozzle exit. Figure 4a shows the five selected mean axial velocity profiles, and Fig. 4b shows the five corresponding mean tangential velocity profiles. As expected, the nonswirling jet has a top-hat profile at the jet exit. However, the swirling jet profiles all exhibit profiles with a peak axial velocity on the centerline. The magnitude of the centerline velocity increases

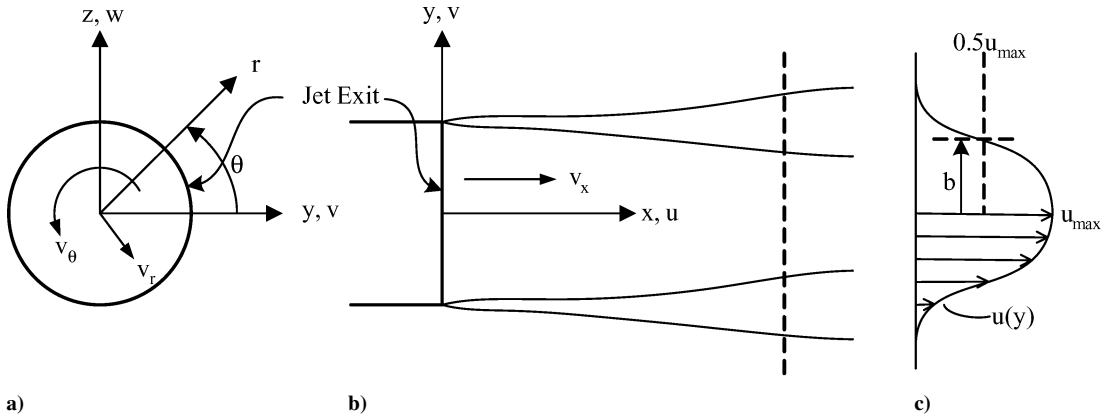

Fig. 3 Schematic of swirling jet showing coordinate system and important parameters: a) view looking from downstream toward the nozzle exit, b) plan view, and c) representation of the axial velocity profile along the dashed line in panel b for $z = 0$.

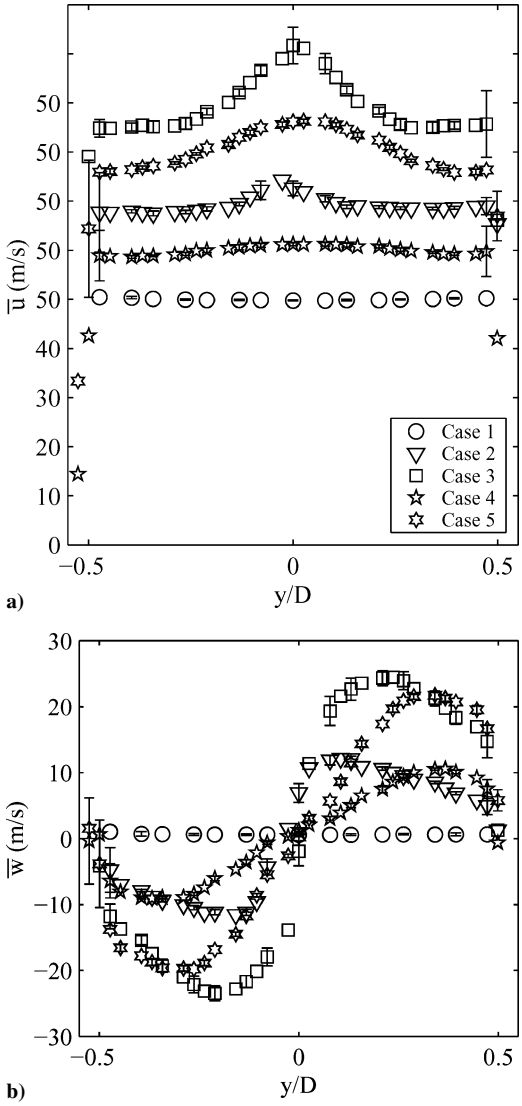

Fig. 4 Mean velocity profiles at the jet exit: a) axial velocity and b) tangential profile. Note that axial velocity profiles have been offset for clarity.

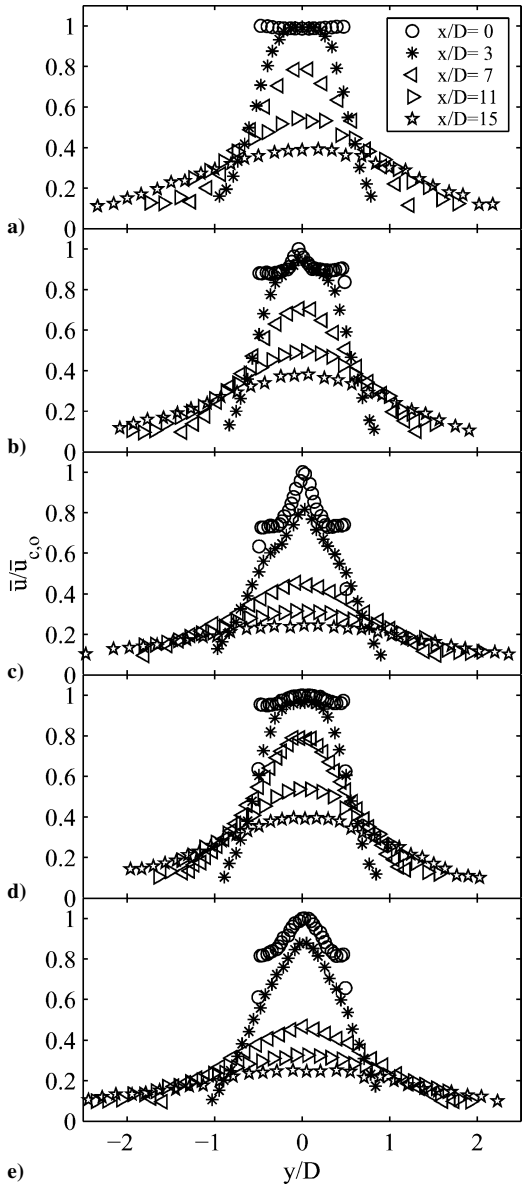

Fig. 5 Normalized mean axial velocity profiles at several axial locations: case a) 1, b) 2, c) 3, d) 4, and e) 5.

with increasing swirl number, and the q-vortex-type swirl has a higher centerline velocity than the solid-body type swirl with the same swirl number. Because of the long mixing length and considerable flow conditioning, the centerline axial velocity peak is not linked to the swirl injection scheme used here. Similar axial velocity profiles have been observed by Farokhi et al.,[3] who also found a higher centerline jet velocity for the q-vortex type profile. Further discussion and an explanation of this phenomenon are provided next.

The mean tangential velocity profiles at the nozzle exit exhibit good symmetry and show that two families of swirling jets have been generated. The two q-vortex-type swirling jets have small cores where the tangential velocity gradient is high. The tangential velocity reaches a maximum a short distance from the axis and decreases with further increases in radius. In contrast, the solid-body-type swirling flows show increasing tangential velocity with radius up to a radial location nearly equal to the nozzle exit radius. Note that the tangential injection has been adjusted to produce the same swirl number for each pair of swirl profiles (one solid-body type and one q-vortex type).

Flowfield Surveys

Although producing the desired swirl profiles has been one of the main challenges of this project, the downstream behavior of the different cases is of greater interest. The normalized axial and tangential velocity profiles and the pressure coefficient profiles are shown at several x/D locations for the different cases of this study in Figs. 5–7. The velocity values used to normalize these profiles are given in Table 1.

The axial velocity profiles exhibit several interesting features. The nonswirling jet (Fig. 5a) has a top-hat mean axial velocity profile $\bar{u}$ at the jet exit and continues to display a potential core until $x/D \approx 5$. At locations further downstream, the nonswirling jet continues to spread as expected. The complex axial velocity profiles with a peak velocity on the centerline exhibited by all of the swirling flows near the nozzle exit rapidly decay into profiles that, for $x/D > 4$, resemble the shape of the nonswirling jet profile. Even though the higher swirl jets have a higher peak velocity on the centerline at the jet exit than the lower swirl jets, the excess axial velocity decays rapidly until the axial velocity profile approaches that of the nonswirling jet for $x/D > 4$ (Fig. 5) suggesting that mixing is vigorous. The peak axial velocity region for the q-vortex-type swirling jet is higher in magnitude and is concentrated near to the core as compared to the broader distribution for the solid-body swirling flow. Note that these swirling jets all have the maximum axial velocity on the centerline indicating that none of the swirl levels is sufficient to produce the centerline velocity decrease necessary for vortex breakdown to occur.

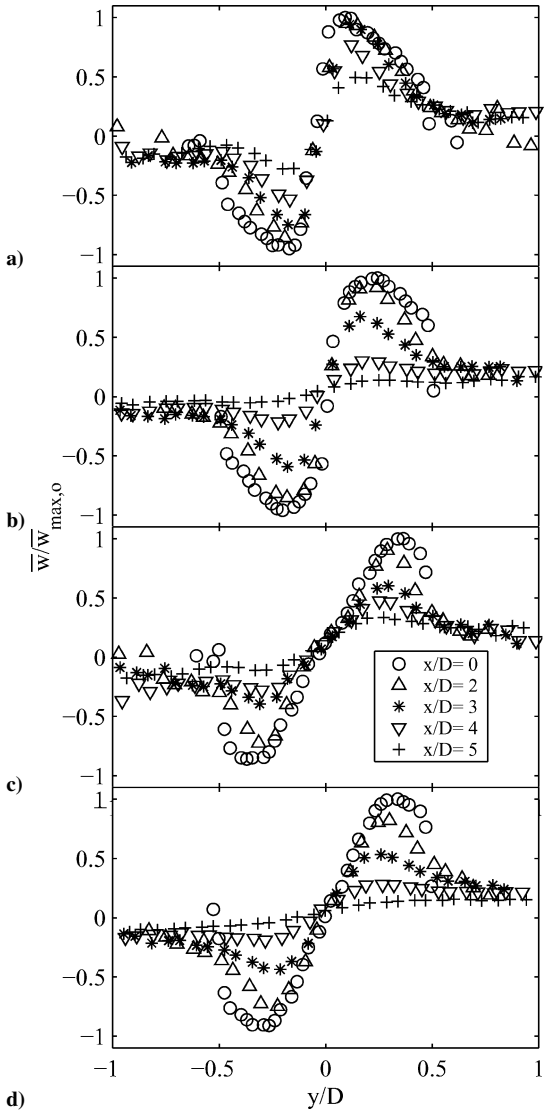

Fig. 6 Normalized mean tangential velocity profiles at several axial locations: case a) 2, b) 3, c) 4, and d) 5. Note that the tangential velocities for the nonswirling jet are small and thus are not shown here.

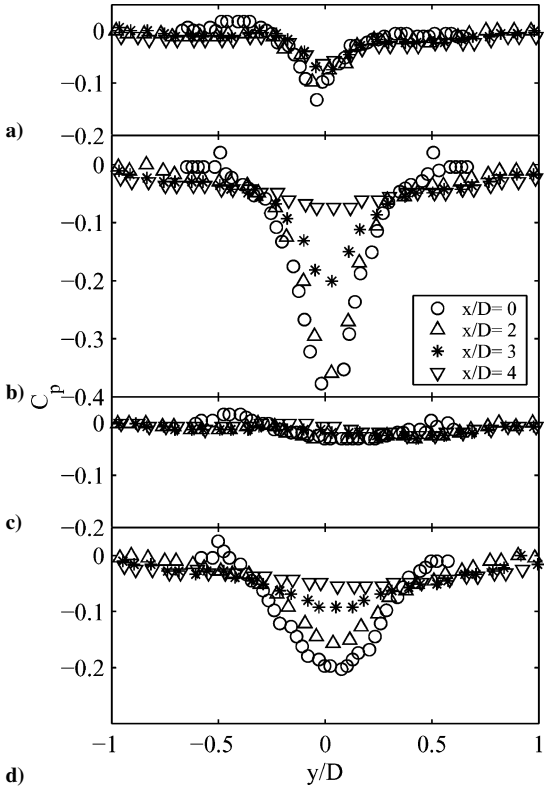

Fig. 7 Pressure coefficient profiles at several axial locations near the jet exit: case a) 2, b) 3, c) 4, and d) 5. Note that the pressure coefficients for the nonswirling jet (case 1) are essentially zero and thus are not shown here.

Panda and McLaughlin[15] provide an explanation of why increased centerline velocities are observed in some swirling jets. When fluid flows containing a uniform axial velocity profile and a significant tangential velocity component pass through a contraction, vortex lines that are initially parallel to the axis turn into spirals. An additional component of vorticity is produced that yields a negative value of $\partial\bar{u}/\partial r$ so that the contraction produces a maximum axial velocity at the centerline. The rapid decay of this axial velocity peak is discussed further in the following.

In contrast to the axial velocity, the tangential velocity profiles change rapidly in the region $0 < x/D < 5$. As a result, the normalized tangential velocities shown in Fig. 6 only include profiles from this region. Note that, along the y axis where the surveys are taken, the z velocity is related to the tangential velocity by $v_\theta = |w|$. The profiles initially change slowly as angular momentum is transferred from the jet to the ambient region outside the jet. The solid-body flows exhibit a transfer of angular momentum from the outer region of the jet, whereas the core region is largely unchanged, which is particularly evident in the higher swirl case. As a result, significant changes in the tangential velocity profile are observed as x increases. The most dramatic result in this figure is the rapid diffusion of angular momentum between two and five diameters. Although all of the cases exhibit this rapid change, it is most evident in the high-swirl cases. Because the swirl levels studied here are below those required for vortex breakdown, some other mechanism must be responsible for this rapid transport of angular momentum. The axial locations where this increased momentum diffusion takes place are in the range where the potential core disappears in the nonswirling case. The behavior of the tangential velocity profiles in the near field ($x/D < 3$) is qualitatively similar to the results of Farokhi et al.[3]

The radial velocities (not shown) are small for all cases. The swirling flows all exhibit small radial outflow velocities that correspond to the decreasing axial velocity. The radial velocities decay with increasing x/D.

Distributions of the pressure coefficient

$$C_p = \frac{\bar{P} - P_a}{0.5\rho U_0^2} \tag{2}$$

are shown in Fig. 7. This figure reveals substantial differences in the pressure distribution that correspond to the type and strength of the swirl. The tangential velocity of the swirling jets requires a radial pressure gradient as indicated by the simplified radial momentum equation for this flow:

$$\frac{\partial P}{\partial r} = \frac{\rho v_\theta^2}{r} \tag{3}$$

As expected, the high-swirl, q-vortex case, which exhibits the highest tangential and axial velocities at the exit, has the lowest core pressures. As the jet proceeds downstream and the tangential velocity decays, the centerline static pressure rises producing an adverse pressure gradient. This adverse pressure gradient acts to slow the axial velocity of the fluid near the core. Similar results were obtained by Farokhi et al.,[3] where increased centerline velocities were observed at the exit of a swirling jet that dissipated within a few diameters downstream. Some of the results from Farokhi et al. show the formation of a wake-like profile (maximum axial velocity occurs off the centerline) further downstream. The current study does not experience wake-like profiles because of the lower swirl levels of the cases investigated, which have swirl numbers on the order

Table 2 Characteristic radius and circulation over $0 \le x/D \le 4$ for the four swirling jet cases

	Case 2		Case 3		Case 4		Case 5	
x/D	r_t, m	k_t, m^2/s	r_t, m	k_t, m^2/s	r_t, m	k_t, m^2/s	r_t, m	k_t, m^2/s
0	0.0060	0.109	0.0068	0.261	0.0129	0.190	0.0112	0.358
1	0.0062	0.108	0.0064	0.246	0.0136	0.187	0.0100	0.200
2	0.0054	0.091	0.0060	0.211	0.0117	0.142	0.0088	0.223
3	0.0048	0.075	0.0055	0.133	0.0197	0.177	0.0084	0.134
4	0.0071	0.079	0.0072	0.067	0.0137	0.079	0.0109	0.082

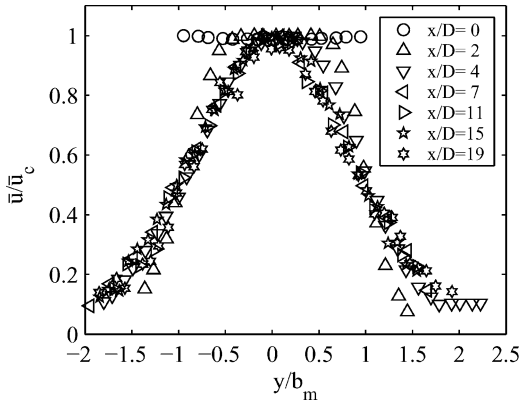

Fig. 8 Normalized axial velocity for nonswirling jet showing collapse of the data for $x/D > 4$.

of one-half and maximum initial pressure coefficient minimums of about 20% of those studied by Farokhi et al.

The nonswirling jet case can be used both as a means for comparison and to ensure that the facility is producing a flow that exhibits characteristics typical of freejets. In Fig. 8, the maximum axial velocity at the exit and jet velocity half-widths b_{hw} have been used to nondimensionalize the axial velocity profiles. The determination of the jet velocity half-width using fits to theoretical profiles is discussed next. As is evident from the figure, the top-hat profile rapidly evolves into a profile typical for a nonswirling jet when normalized appropriately. For $x/D > 4$, the data appear to collapse.

In an attempt to characterize the swirling flows in more depth than provided by the swirl number alone, a normalized circulation has been calculated. Hoffman and Joubert have postulated that there is a universal circulation distribution for fully turbulent vortices.[33] Figure 9 shows the normalized circulation at several different axial locations plotted against a normalized radius for the four swirling cases. A normalized circulation of unity, as indicated by the dashed line in the figure, is the asymptotic behavior of a swirling flow that exhibits $v_\theta \propto r^{-1}$, whereas a circulation of $k/k_t = r^2/r_t^2$, indicated by the solid line in the figure, represents solid-body rotation where $v_\theta \propto r$. Only a portion of the circulation distribution is plotted here because, in the near field, the mixing layer causes the distribution to deviate from the "universal" distribution. As expected, the q-vortex flows begin to reach a $k/k_t = 1$ more rapidly than do the solid-body flows. This occurs because only the edge of the solid-body jet displays a $v_\theta \propto r^{-1}$ behavior at the jet exit, whereas all but the core of the q vortex displays a $v_\theta \propto r^{-1}$ relationship at the jet exit. Despite the difference between the four flows, it is clear that they can all be represented by a certain combination of $v_\theta \propto r^{-1}$ and $v_\theta \propto r$ behavior.

The circulation k_t and the core radius r_t used to characterize the four swirling cases are tabulated in Table 2. The characteristic radii of the solid-body swirl cases are higher than those of the q-vortex cases as expected. An interesting feature is that, with the exception of the low-swirl solid-body case (case 4), the characteristic radius decreases up to $x/D = 3$ and then increases substantially. In the higher-swirl cases, this increase in characteristic radius is accompanied by a large decrease in k_t. This result supports the preceding observation that a significant change in the tangential velocity profiles is experienced between three and five diameters downstream of the nozzle exit.

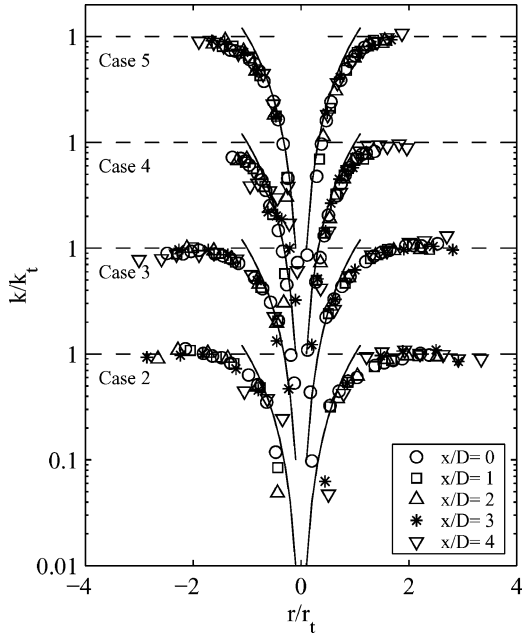

Fig. 9 Normalized circulation of the four swirl cases. Note that the curves have been offset for clarity.

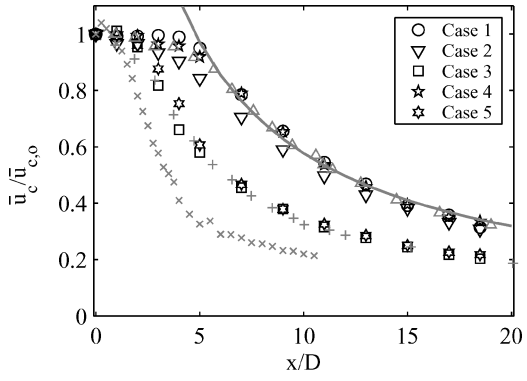

Fig. 10 Centerline velocity normalized by the centerline velocity at the jet exit for the five different cases. The results shown in gray are from previous studies: △, Rose,[12] $S = 0$; +, Rose,[12] $S = 0.2$; ×, Farokhi et al.,[3] $S = 0.48$; and ——, theory,[34] $S = 0.0$.

Jet Growth

To address the primary goal of this study, the assessment of the effect of initial swirl profile on growth rate, means of determining the jet growth are necessary. Because of the complex nature of the axial velocity profile for $x/D < 5$, the direct application of methods used to determine jet growth in nonswirling jets to the present swirling cases is not always valid. Traditional methods of determining jet growth include the centerline decay rate and the jet thickness as defined by the point where the velocity drops to some fraction of the centerline velocity. However, both of these methods can lead to erroneous results because of the complex axial velocity profiles observed in the swirling jets. For example, Fig. 10 shows the decay rate of the centerline velocity normalized by the centerline velocity

at the nozzle exit along with results from Farokhi et al.[3] and Rose[12] as well as the theoretical result.[34] Note that the velocity decay for the present nonswirling jet agrees well with the theoretical curve

$$\frac{\bar{u}_c}{\bar{u}_{c,o}} = \frac{0.96 * R}{a(x - s)} \tag{4}$$

where a and s are constants that govern the rate of decay and offset from the jet exit for a particular case. The values of these constants for the present study, $a = 0.067$ and $as/R = 0.31$, are close to those found in previous studies.[34] The present results also agree surprisingly closely with those of the nonswirling and swirling ($S = 0.20$) data from Rose.[12] The centerline decay rate from Farokhi et al.[3] is also shown and exhibits a higher decay rate caused by a higher swirl number ($S = 0.48$). From this figure, it appears that the low-swirl cases have little effect on jet growth, whereas the high-swirl cases yield an identical increase in jet growth. However, the q vortex has a higher centerline velocity at the exit that affects the results. Because of features such as this, an approach that considers the entire velocity distribution is required.

To determine a jet growth rate that addresses the complex axial velocity profiles found in swirling jets, a momentum-based method has been developed. In this method, the axial momentum flux and pressure force at the jet exit are summed:

$$\int_0^R 2\pi r \rho \bar{u}^2(r, x = 0)\, \mathrm{d}r + \int_0^R 2\pi r [\bar{P}(r, x = 0) - P_a]\, \mathrm{d}r \tag{5}$$

At locations downstream of the exit, the jet momentum half-width is defined as the radial distance within which is contained a certain percentage of the momentum flux and pressure force present at the nozzle exit. At each x location, the momentum half-width b_m is determined by increasing r until

$$\frac{\int_0^r 2\pi r \rho \bar{u}^2(r)\, \mathrm{d}r + \int_0^r 2\pi r [\bar{P}(r) - P_a]\, \mathrm{d}r}{\int_0^R 2\pi r \rho \bar{u}^2(r, x = 0)\, \mathrm{d}r + \int_0^R 2\pi r [\bar{P}(r, x = 0) - P_a]\, \mathrm{d}r} = c \tag{6}$$

where c is a constant between 0 and 1. Here, c has been chosen to be 0.6. The static-pressure term is included to account for the pressure-gradient effects that are present in the flow because the static pressure is not constant in the swirling jets as just discussed. Interpolation between the experimental data points is used to increase the accuracy of the momentum half-width estimate. Error estimates for the momentum half-widths are determined by propagating the uncertainties of the axial velocities through Eq. (6). The upper and lower bounds of the integrated momentum flux and pressure force near the radius where Eq. (6) is satisfied are used to estimate the error in the momentum half-width b_m. Note that the uncertainty of the momentum half-widths is typically less than 4%.

The jet momentum half-widths determined using the method just outlined are shown in Fig. 11 in the near-exit region ($x/D < 5$).

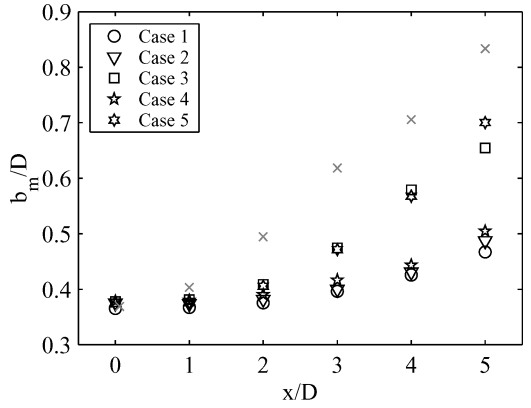

Fig. 11 Jet momentum half-width for $x/D < 5$ for the five different cases. Also shown in gray are momentum half-widths determined from the data of Farokhi et al.[3] ($\times$) for $S = 0.48$.

Note that the uncertainties have not been plotted to avoid obscuring the behavior of the different cases. Two points that are immediately obvious are that the low-swirl cases do little to enhance jet growth, whereas the high-swirl cases achieve a significant and sustained enhancement. The results from Farokhi et al.[3] (Farokhi, S., private communication, April 2004) for a solid-body type swirl with $S = 0.48$ are also shown in Fig. 11. The q-vortex-type distribution from the same study is not shown because it was on the verge of vortex breakdown, which affected the results accordingly. Another trend that appears in this figure is that, although all of the jets start with essentially the same momentum half-width, the more swirl the jets contain, the sooner their widths deviate from the nonswirling jet result. The jets with higher swirl not only exhibit larger widths for the same x/D, but they also display an increased growth rate. The initial swirl distribution does not appear to play a large role in the increased momentum half-widths shown.

Based on the observation that the axial velocity profiles for the swirling cases rapidly approach the distribution associated with nonswirling jet flows, jet velocity half-widths have also been determined by fitting the axial velocity profiles with a theoretical jet profile[35]

$$\bar{u}/\bar{u}_c = \mathrm{sech}^2[a(r/x)] \tag{7}$$

Although this form is often associated with axial velocity profiles of two-dimensional jets, it has been shown that it provides an excellent fit for axisymmetric jets provided the constants are modified. The jet velocity half-width is defined here as half the distance between the locations where the axial velocity drops to half of the centerline velocity (i.e., $\bar{u}_c/2$). Evidence that this approach is valid for $x/D > 4$ is provided by Fig. 12, which shows that the downstream axial velocity profiles collapse well when nondimensionalized with the half-velocity half-width b_{hw}. The uncertainty in the jet velocity half-width is determined from the 95% confidence interval for the velocity predicted using Eq. (7) in the region near the half-velocity point. Typical uncertainties in the jet velocity half-width determined using this fit method are less than 5%.

The jet velocity half-widths determined using this fitting method b_{hw} are shown at different axial locations in Fig. 13. Note that only b_{hw} values are plotted only for $x/D \geq 4$ because the axial velocity profiles of the swirling jets before this location have yet to relax to a nonswirling jet profile for which the Eq. (7) is a good representation. Again, the uncertainties have not been shown in the figure to improve clarity. As with the momentum half-width b_m in the near field, the velocity half-width b_{hw} shows little difference between the nonswirling cases and the $S = 0.10$ swirling cases up to $x/D \sim 20$. The velocity half-widths for the higher swirl cases also collapse to

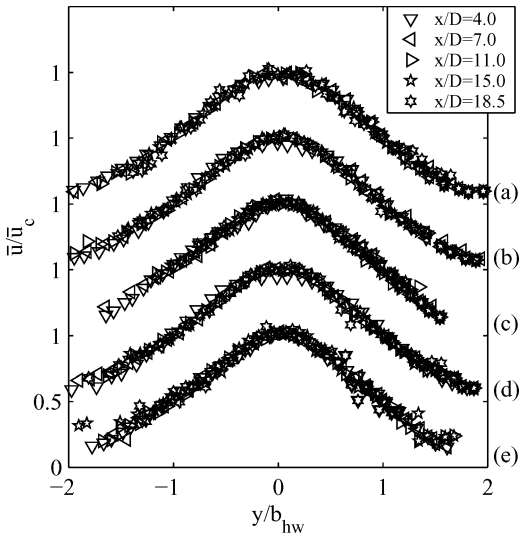

Fig. 12 Normalized jet velocities using the velocity half-width (determined using sech^2 fit) to nondimensionalize y. Note that each case is offset for clarity: case a) 1, b) 2, c) 3, d) 4, and e) 5.

Table 3 Growth rates for the nonswirling and swirling jet cases

Case	b'_{hw}	$b'_{\mathrm{hw}}/b'_{\mathrm{hw},S=0}$
1	0.096 ± 0.005	1.00 ± 0.08
2	0.094 ± 0.004	0.97 ± 0.07
3	0.134 ± 0.006	1.39 ± 0.10
4	0.089 ± 0.005	0.93 ± 0.07
5	0.130 ± 0.011	1.35 ± 0.14

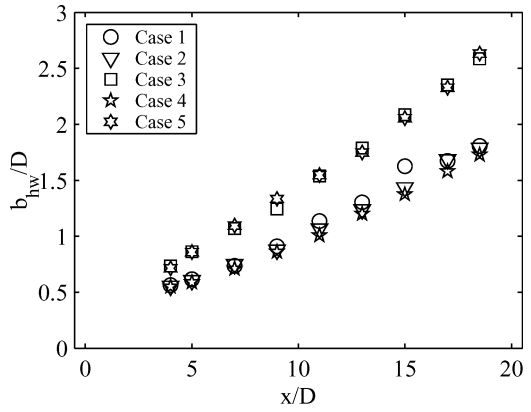

Fig. 13 Jet velocity half-width determined using sech^2 fit for the five different cases.

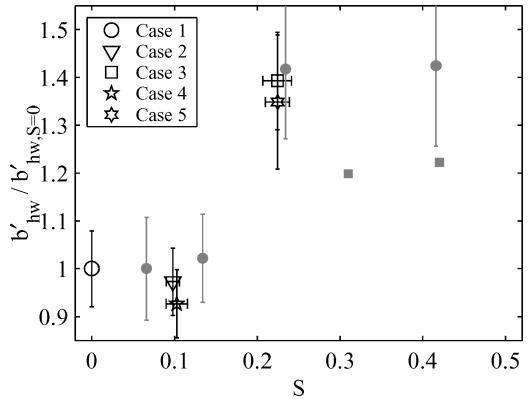

Fig. 14 Normalized growth rate for the four swirling cases determined from the velocity half-width found using the sech^2 curve fit. Data in gray are from previous studies: ●, Chigier and Chervinsky[14] and ■, Elsner and Kurzak.[17]

a single curve with significantly higher widths than the lower swirl and nonswirling cases.

To quantify the growth-rate enhancement effectiveness of the different swirling jets, a growth rate is determined by performing a linear fit to the data in the developing region ($x/D > 5$). The slope of this line $b' = \mathrm{d}b/\mathrm{d}x$ is the growth rate, and, if nondimensionalized by the growth rate of the nonswirling jet $b'_{S=0}$, the normalized growth rate can be determined. This normalized growth rate is a quantification of the enhancement caused by swirl. The uncertainties for the growth rates are determined from the uncertainties associated with the half-widths using the linear regression uncertainty approach discussed by Brown et al.[36] (also see Ref. 37).

Table 3 summarizes the absolute growth rates and the normalized growth rates obtained using velocity half-widths determined using the sech^2 fits, and Fig. 14 shows the normalized growth rates as a function of swirl number S. Also shown in the figure are growth rates determined from half-widths calculated from Chigier and Chervinsky's original velocity data,[14] and half-widths reported by Elsner and Kurzak for a slightly heated jet.[17] As indicated by the half-width results, the low-swirl cases produce no measurable enhancement of growth rate over the nonswirling case, whereas the high-swirl cases significantly increase the growth rate. In addition, the effect of initial swirl distribution appears to play little role in the mixing the enhancement observed. Both velocity half-widths and growth rates (not shown in Fig. 13) calculated from the data of Chigier and Chervinsky are higher than the results of the current study and exhibit a greater amount of scatter than the data of the present study. However, the ratios of the growth rates with swirl to that without swirl produce results that fall in line with the present results. In contrast, Elsner and Kurzak's growth rate ratios are well below those of the present study as are the half-widths they report. The reason for this discrepancy is not clear at this point. However, both of these data sets seem to indicate a saturation of the enhancement effect at some swirl level prior to the swirl level required for vortex breakdown. The saturation is suggested by the flattening of the curves in the range $0.25 < S < 0.45$.

Growth rates have also been calculated from the momentum half-widths in the developing region for the cases of the present study. The results are similar to those determined from the velocity half-widths, but a slight difference in enhancement is found between the q-vortex and solid-body distributions. Because the axial velocity profiles are well represented by sech^2 fit in the developing region and the velocity half-width is a more common measure of jet width, the velocity half-width results are preferred here.

Discussion

The results of this study confirm many previous observations in swirling jets and reveal some new features. A presentation of the most important of these findings and placement in the context of previous work are provided here.

The centerline decay rates of the swirling jets studied here have been compared to results obtained in other facilities and agree surprisingly well. Regardless of the swirl generation mechanism and flow conditioning, the centerline decay rate seems to be accurately predicted by the swirl number. This suggests that the dynamics of the mixing process are dominated by swirl effects, and other factors play only a secondary role.

Because of concerns of using centerline velocity decay rates to estimate swirling jet growth caused by complex axial velocity profiles, two approaches for estimating a jet half-width that consider part or all of the axial velocity profile have been presented here. These two methods produce slightly different estimates of the normalized jet growth rate as a result of their definitions. The momentum half-width method addresses the complex axial velocity and pressure profiles found in the near-exit and transition regions by integrating the momentum flux and pressure force and comparing the result to the value at the nozzle exit. This is perhaps one of the few ways to provide an unbiased estimate of jet width in the near field. However, this approach links its results to conditions at the nozzle exit. In contrast, the velocity half-width approach only considers what happens in the far field (i.e., it is not coupled to the exit conditions), but it only works where the axial velocity profiles have relaxed to the fully developed profile typical of a jet. The choice of which method to use depends on the region of interest.

From the growth rates predicted using the velocity half-width in the developing region, it does not appear that the growth rates are highly sensitive to the initial tangential velocity distribution for the cases tested. By five diameters downstream of the nozzle exit, the tangential velocity distributions are similar, and the tangential velocity magnitudes have decayed significantly from their exit values. This rapid change in swirl distribution is not completely understood, but it appears that the mixing processes are extracting energy from the tangential velocity profiles because they decay at much higher rates than the axial velocity profiles.

Although the tangential velocity profile does not appear to play a large role in the growth rates observed, the magnitude of the swirl does. The lower swirl cases studied here have no effect on the growth rate observed, whereas the larger swirl cases have a significant effect. The observation of the ineffectiveness of low swirl on enhancing mixing has been observed before in the near field of a swirling jet.[13] The threshold swirl for the onset of jet-growth enhancement and an optimum swirl remain to be determined.

From the jet half-width results presented here, there appear to be three regions of importance: a near-field region, a transition region, and a developing region. In the near field, $x/D < 1-2$, the growth rates of all of the jets are small, and the tangential velocity profiles remain well defined and distinct from each other. It is likely that, in this region, the instabilities that produce the increased growth rate observed downstream first begin to amplify. In the transition region, $1-2 < x/D < 5$, the tangential velocity profiles experience a rapid increase in characteristic radius and a rapid decrease in circulation. This corresponds to a rapid decrease in tangential velocity and a substantial redistribution of the remaining angular momentum. In the same region, the half-widths of the jets with different swirl numbers start to diverge and grow nonlinearly. It is likely that the turbulent structures generated from instabilities in the near-field undergo complex interactions with each other and the mean flow in this region thereby causing the significant growth enhancement observed. In the developing region, $x/D > 5$, the tangential velocities essentially disappear. However, the increased growth rates associated with the higher swirl cases that started in the transition region persist and become linear even in the absence of a significant swirl component. This suggests that the structure generated in the near field that evolves in the transition region persists in the developing region and continues to enhance jet growth.

Although the measurements completed in this study do not identify the mechanism responsible for enhanced jet growth in swirling jets, they do provide some important insight. The bulk Richardson number, a measure of centrifugal instability, indicates instability when it drops below zero. The swirling jets studied here have negative Richardson numbers only in a small region at the periphery of the jet where the tangential velocity drops to zero. Although this suggests that centrifugal effects might play a role in the enhanced jet growths observed here, this study again shows that a highly unstable mean velocity profile is not necessary for enhancement. As suggested by other studies, it is likely that the tangential shear is the more likely cause of the enhanced growth rates observed. Although the magnitude of the tangential velocity and the resultant shear rapidly drop with increasing x/D, there is sufficient shear in the near field and transition regions to create a turbulent structure that persists downstream and continues to enhance jet growth.

Several of the results from this study appear to support results from computational work. Linear stability theory has shown that a finite amount of swirl is necessary to excite negative helical modes. The ineffectiveness of the low swirl for jet growth enhancement in this study supports this result. The higher growth rates for the helical modes and potential transition from convective to absolute instability at finite swirl numbers are also supported by the results of this study. However, it is the rapid growth of the mixing layer and corresponding decay of tangential velocity in the transition region of the jet that support the results from DNS studies that suggest an interaction between structures in the shear layer and the jet swirl. Further DNS studies investigating a swirling jet's response to a broad range of instabilities can clarify this result.

Conclusions

An experimental study has been carried out to study the effect of swirl on growth-rate enhancement in incompressible jets. This study differs from earlier work in that highly conditioned swirling jets with two distinctive tangential velocity profiles, a solid-body and a q-vortex type, and two different swirl numbers that are well below that required for vortex breakdown have been investigated in a single study. The present data are also useful for computational validation as a result of the low uncertainties and the level of control maintained in the experiments. The results of this study indicate that the role of the tangential velocity distribution (i.e., solid body vs q-vortex type) in the growth-rate enhancement is not great. All tangential velocity profiles rapidly decay and approach a similar distribution only a few diameters downstream of the exit. As swirl levels sufficient for vortex breakdown are approached, the tangential velocity distribution will play an important role (see Farokhi et al.[3] as an example).

In contrast to the tangential velocity distribution, the degree of swirl (characterized by the swirl number) is found to have an important effect on growth-rate enhancement. In contrast to earlier work that suggested that the growth rate grows linearly with swirl number (up to some finite level of swirl),[14] this study has yielded enhanced growth rates in the developing region (up to 40% for the cases studied) only when the swirl number exceeds a certain value. This result extends similar observations in previous studies of the near field[13] to the developing region. As a result, there appear to be at least three different regions of swirl-enhanced jet growth rate: 1) $S < 0.1$ where there is no enhancement effect, 2) $0.1 < S < 0.3$ where enhancement scales with swirl, and 3) where the swirl number is sufficiently high for vortex breakdown to occur and vortex breakdown dominates the process. Other studies' results also indicate that the growth-rate enhancement might saturate before a swirl number sufficient for vortex breakdown is reached. The exact swirl levels defining the borders of these regions is not known and should be the subject of a future investigation.

A surprising result is that the extensive flow conditioning applied in this study did not appear to have the expected effect on the mean results. The current results agree well with previous results from facilities in which artifacts from swirl generation and nontypical nozzle exit conditions were likely present. This suggests that the dynamics created by the presence of swirl dominate the mixing process and the exit conditions only play a secondary role.

The current results raise as many questions as they answer. To understand the enhanced growth rates observed for $x/D > 5$, measurements of fluctuating velocities are required. Although such measurements would provide evidence that enhancement is present and how it is manifested, the mechanism behind the enhanced growth rates requires identification of how the turbulent structure is modified. Because these structures are responsible for jet mixing and growth, only by identifying how they are modified in the presence of swirl will this growth enhancement process be fully understood. With an understanding of how the turbulent structure is modified, swirl or some other similar enhancement technique can be exploited for control purposes.

Acknowledgments

This work has been primarily supported through the Air Force Office of Scientific Research under Grant F49620-00-1-0255. Steven Walker and John Schmisseur have been the Technical Monitors. We thank the reviewers for their comments that improved the manuscript substantially.

References

[1]Farokhi, S., Taghavi, R., and Rice, E. J., "Modern Developments in Shear Flow Control with Swirl," *AIAA Journal*, Vol. 30, No. 6, 1992, pp. 1482–1483.

[2]Naughton, J. W., Cattafesta, L. N., and Settles, G. S., "An Experimental Study of Compressible Turbulent Mixing Enhancement in Swirling Jets," *Journal of Fluid Mechanics*, Vol. 330, 1997, pp. 271–305.

[3]Farokhi, S., Taghavi, R., and Rice, E. J., "Effect of Initial Swirl Distribution on the Evolution of a Turbulent Jet," *AIAA Journal*, Vol. 27, No. 6, 1989, pp. 700–706.

[4]Hu, G.-H., Sun, D.-J., and Yin, X.-Y., "A Numerical Study of Dynamics of a Temporally Evolving Swirling Jet," *Physics of Fluids*, Vol. 13, No. 4, 2001, pp. 951–965.

[5]Sun, D.-J., Hu, G.-H., Gao, Z., and Yin, X.-Y., "Stability and Temporal Evolution of a Swirling Jet with Centrifugally Unstable Azimuthal Velocity," *Physics of Fluids*, Vol. 14, No. 11, 2002, pp. 4081–4084.

[6]Loiseleux, T., Chomaz, J. M., and Huerre, P., "The Effect of Swirl on Jets and Wakes: Linear Instability of the Rankine Vortex with Axial Flow," *Physics of Fluids*, Vol. 10, No. 5, 1998, pp. 1120–1134.

[7]Olendraru, C. O., Sellier, A., Rossi, M., and Huerre, P., "Inviscid Instability of the Batchelor Vortex: Absolute-Convective Transition and Spatial Branches," *Physics of Fluids*, Vol. 11, No. 7, 1999, pp. 1805–1820.

[8]Gilchrist, R. T., and Naughton, J. W., "The Design of a Swirling Jet Facility," AIAA Paper 2002-0442, 2002.

[9]Beer, J. M., and Chigier, N. A., *Combustion Aerodynamics*, Krieger, Malabar, FL, 1983, Chap. 5.

[10]Gupta, A. K., Lilley, D. G., and Syred, N., *Swirl Flows*, Abacus Press, Kent, England, U.K., 1984, Chaps. 1 and 3.

[11]Bradshaw, P., "Effects of Streamline Curvature on Turbulent Flow," AGARDograph 169, Aug. 1973.

[12]Rose, W. G., "A Swirling Round Turbulent Jet," *Journal of Applied Mechanics, ASME Transactions, Series E*, Vol. 84, Dec. 1962, pp. 615–625.
[13]Mehta, R. D., Wood, D. H., and Clausen, P. D., "Some Effects of Swirl on Turbulent Mixing Layer Development," *Physics of Fluids A*, Vol. 3, No. 11, 1991, pp. 2717–2724.
[14]Chigier, N. A., and Chervinsky, A., "Experimental Investigation of Swirling Vortex Motion in Jets," *Journal of Applied Mechanics*, June 1967, pp. 443–451.
[15]Panda, J., and McLaughlin, D. K., "Experiments on the Instabilities of a Swirling Jet," *Physics of Fluids*, Vol. 6, No. 1, 1994, pp. 263–276.
[16]Cutler, A. D., Levey, B. S., and Kraus, D. K., "Near-Field Flow of Supersonic Swirling Jets," *AIAA Journal*, Vol. 33, No. 5, 1995, pp. 876–881.
[17]Elsner, J., and Kurzak, L., "Characteristics of Turbulent Flow in Slightly Heated Free Swirling Jets," *Journal of Fluid Mechanics*, Vol. 180, July 1987, pp. 147–169.
[18]Mattingly, J. D., and Oates, G. C., "An Experimental Investigation of the Mixing of Coannular Swirling Flows," *AIAA Journal*, Vol. 24, No. 5, 1986, pp. 785–792.
[19]Chen, R.-H., Driscoll, J. F., Kelly, J., Mamazian, M., and Schefer, R. W., "A Comparison of Bluff-Body and Swirl-Stabilized Flames," *Combustion Science and Technology*, Vol. 71, No. 4–6, 1990, pp. 197–217.
[20]Lessen, M., Singh, P. J., and Paillet, F., "The Stability of a Trailing Line Vortex. Part 1. Inviscid Theory," *Journal of Fluid Mechanics*, Vol. 63, No. 4, 1974, pp. 753–763.
[21]Lessen, M., and Paillet, F., "The Stability of a Trailing Line Vortex. Part 2. Viscous Theory," *Journal of Fluid Mechanics*, Vol. 65, No. 4, 1974, pp. 769–779.
[22]Khorrami, M. R., "On The Viscous Modes of Instability of a Trailing Line Vortex," *Journal of Fluid Mechanics*, Vol. 225, 1991, pp. 197–212.
[23]Khorrami, M. R., "Stability of a Compressible Axisymmetric Swirling Jet," *AIAA Journal*, Vol. 33, No. 4, 1995, pp. 650–658.
[24]Cooper, A. J., and Peake, N., "The Stability of a Slowly Diverging Swirling Jet," *Journal of Fluid Mechanics*, Vol. 473, 2002, pp. 389–411.
[25]Lu, G., and Lele, S., "Inviscid Instability of Compressible Swirling Mixing Layers," *Physics of Fluids*, Vol. 11, No. 2, 1999, pp. 450–461.
[26]Delbende, I., Chomaz, J.-M., and Huerre, P., "Absolute/Convective Instabilities in the Batchelor Vortex: A Numerical Study of the Linear Impulse Response," *Journal of Fluid Mechanics*, Vol. 355, Jan. 1998, pp. 229–254.
[27]Younis, B. A., Gatski, T. B., and Speziale, C. G., "Assessment of the SSG Pressure-Strain Model in Free Turbulent Jets with and Without Swirl," *Journal of Fluids Engineering*, Vol. 118, 1996, pp. 800–809.
[28]Chen, R. H., and Driscoll, J. F., "The Role of Recirculation in Improving Internal Mixing," *Proceedings of the Combustion Institute*, Vol. 22, 1988, pp. 531–540.
[29]Wu, C., and Farokhi, S., "Spatial Instability of a Swirling Jet—Theory and Experiment," *AIAA Journal*, Vol. 30, No. 6, 1992, pp. 1545–1552.
[30]Chow, J. S., Zilliac, G. G., and Bradshaw, P., "Measurments in a Wingtip Vortex," *AIAA Journal*, Vol. 35, No. 10, 1997, pp. 1561–1567.
[31]Samet, M., and Einav, S., "Mean Value Measurements of a Turbulent Swirling-Jet," *AIAA Journal*, Vol. 26, No. 5, 1988, pp. 619–621.
[32]Zilliac, G. G., "Modelling, Calibration, and Error Analysis of Seven-Hole Pressure Probes," *Experiments in Fluids*, Vol. 14, No. 1/2, 1993, pp. 104–120.
[33]Hoffman, E. R., and Joubert, P. N., "Turbulent Line Vortices," *Journal of Fluid Mechanics*, Vol. 16, 1963, pp. 395–411.
[34]Abramovich, G. N., *The Theory of Turbulent Jets*, MIT Press, Cambridge, MA, 1963, pp. 82–85.
[35]White, F. M., *Viscous Fluid Flow*, 2nd ed., McGraw–Hill, New York, 1991, p. 474.
[36]Brown, K. K., Coleman, H. W., and Steele, W. G., "A Methodology for Determining Experimental Uncertainties in Regressions," *Journal of Fluids Engineering*, Vol. 120, No. 3, 1998, pp. 445–456.
[37]Coleman, H. W., and Steele, W. G., *Experimentation and Uncertainty Analysis for Engineers*, 2nd ed., Wiley, New York, 1999, pp. 208–213.

W. Dahm
Associate Editor